Biochimica et Biophysica Acta 1854 (2015) 860–868

Contents lists available at ScienceDirect

Biochimica et Biophysica Acta

journal homepage: www.elsevier.com/locate/bbapap

Mutation of Gly717Phe in human topoisomerase 1B has an effect on enzymatic function, reactivity to the camptothecin anticancer drug and on the linker domain orientation

Zhenxing Wang [a,1], Ilda D'Annessa [a,1], Cinzia Tesauro [a,2], Stefano Croce [a], Alessio Ottaviani [a], Paola Fiorani [b,*], Alessandro Desideri [a,*]

[a] Department of Biology, University of Rome Tor Vergata, Via Della Ricerca Scientifica, Rome 00133, Italy
[b] Institute of Translational Pharmacology, National Research Council, CNR, Via Del Fosso del Cavaliere 100, 00133 Rome, Italy

ARTICLE INFO

Article history:
Received 22 October 2014
Received in revised form 27 March 2015
Accepted 15 April 2015
Available online 22 April 2015

Keywords:
Topoisomerase 1B
Camptothecin
Molecular dynamics
Drug resistance

ABSTRACT

Human topoisomerase 1B controls the topological state of supercoiled DNA allowing the progression of fundamental cellular processes. The enzyme, which is the unique molecular target of the natural anticancer compound camptothecin, acts by cleaving one DNA strand and forming a transient protein–DNA covalent adduct. In this work the role of the Gly717 residue, located in a α-helix structure bridging the active site and the linker domain, has been investigated mutating it in Phe. The mutation gives rise to drug resistance *in vivo* as observed through a viability assay of yeast cells. *In vitro* activity assays show that the mutant is characterized by a fast religation rate, only partially reduced by the presence of the drug. Comparative molecular dynamics simulations of the native and mutant proteins indicate that the mutation of Gly717 affects the motion orientation of the linker domain, changing its interaction with the DNA substrate, likely affecting the strand rotation and religation rate. The mutation also causes a slight rearrangement of the active site and of the drug binding site, providing an additional explanation for the lowered effect of camptothecin toward the mutant.

1. Introduction

DNA topoisomerases are key enzymes that modulate the topological state of DNA through the breaking and rejoining of DNA strands. These enzymes have been shown to be essential in all processes of DNA metabolism such as replication, transcription, recombination and chromosomal segregation and are key enzymes as molecular target for anticancer and anti-microbial therapies [1–3]. Due to its importance the human enzyme has been extensively studied during the last decades in order to detect the role of the different domains that compose the protein, both in terms of activity and drug sensitivity [4,5]. Human topoisomerase 1 (hTop1) is a 765 residues protein of 91 kDa that exerts its action by cleaving one strand of the DNA through a tyrosine residue that operates a nucleophilic attack on the strand, supported by four positive residues that altogether form the catalytic pentad (Arg488, Lys532, Arg590, His632 and Tyr723). The protein is composed by an N-terminal domain dispensable for the catalytic activity (residues 1–214), a core domain divided in subdomain I (215–232; 320–433), II (233–319) and III (434–635), a linker domain (636–712) and a C-terminal domain (713–765) [3]. Subdomains I and II form the CAP region, while subdomain III and C-terminal form the CAT region containing the active site, the two regions forming a "clamp" structure that wraps around the DNA substrate, with the linker domain protruding outside of the globular shape of the protein, as shown by the different X-ray structures of the protein solved in non-covalent or covalent complex with the nucleic acid in the presence or the absence of inhibitors [6–10]. HTop1 has been studied since the early 80s, when it was discovered to be inhibited by the natural compound camptothecin (CPT) [11], whose derivatives topotecan and irinotecan have been approved by the FDA for clinical use in anticancer therapy [12]. CPT binds the covalent Top1–DNA complex, slowing down the religation of the cleaved DNA strand. The binding of CPTs to the cleavage complex is *per se* reversible, but the compound becomes lethal due to the collision of the stalled enzyme–DNA complex with the replication fork [5,10,13].

Point mutations that affect the enzyme reactivity to CPT have been deeply analyzed. Most of the mutations that affect CPT sensitivity are located either in the drug binding site or on the linker domain [14–19].

Abbreviations: hTop1B, human topoisomerase 1B; CPT, camptothecin; TPT, topotecan; DMSO, dimethyl sulfoxide; EDTA, ethylenediaminetetraacetic acid; EGTA, ethylene glycol tetraacetic acid; DTT, dithiothreitol; BSA, bovine serine albumin; TBE, tris-borate-EDTA; PMSF, phenylmethanesulfonylfluoride

* Corresponding authors at: Department of Biology, University of Rome Tor Vergata, Via Della Ricerca Scientifica, Rome 00133, Italy.
E-mail addresses: paola.fiorani@uniroma2.it (P. Fiorani), desideri@uniroma2.it (A. Desideri).
[1] These authors contributed equally to the work.
[2] Present address: Department of Molecular Biology and Genetics, University of Aarhus, C.F Møllers Allè 3 8000 Aarhus C, Denmark.

http://dx.doi.org/10.1016/j.bbapap.2015.04.017
1570-9639/

The flexibility of the linker can regulate the religation process affecting CPT sensitivity [17], as reported for the Ala653Pro mutant characterized by an enhanced linker mobility and a fast religation that likely doesn't allow the cleavage complex to be enough persistent to permit the interaction with the drug. In agreement, the double Asp677Gly/Val703Ile mutant, hypersensitive to CPT shows a low religation rate coupled to reduced linker mobility [18]. However it has been shown that CPT resistance is not only correlated to enhanced linker mobility but, as demonstrated for Thr729Lys/Pro, Glu710Gly and Arg634Ala mutants, also to a perturbation of motion correlation between the linker and the C-terminal domain, containing the active site tyrosine [20–22]. These data indicate that the linker domain and the active site of the protein, even if far one from the other, are able to communicate so that a mutation on the linker may have an effect on the active site. The communication goes in both directions since a mutation of a residue close to the active site is also able to perturb the linker flexibility as observed in the Thr718Ala mutant [23].

The importance of the linker has been underlined also in the yeast enzyme that has a linker longer than the human one. Van der Merwe and Bjornsti have shown that mutation of Gly721Phe in yeast Top1 gives rise to a CPT resistant mutant and they hypothesized that this could be due to enhanced linker flexibility, but they did not go through the analysis of the different steps of the catalytic cycle [24]. Motivated from these results we have now mutated in hTop1 the Gly717 residue, that on the basis of the alignment corresponds to Gly721 of the yeast enzyme and the Gly717Phe mutant has been analyzed through a coupled functional and computational analysis to understand its behavior at molecular level. We have specifically selected the Gly717Phe mutation since we hypothesized that introduction of a large lateral chain could strongly perturb the structural dynamical–functional properties of the enzyme. We confirm that the mutation confers CPT resistance, underlining the similarity between the yeast and the human enzyme, and we demonstrate that the mutation induces a fast religation rate likely correlated to a different orientation of the linker domain and a slight rearrangement of the active site as observed by molecular dynamics simulation.

2. Materials and methods

2.1. Chemicals, yeast strains and plasmids

Dimethyl sulfoxide (DMSO) and camptothecin (CPT) were purchased from Sigma-Aldrich. CPT was dissolved in 99.9% DMSO to a final concentration of 4 mg/mL (11.5 mM) and stored at −20 °C. Oxindolimine copper(II) compound ($[Cu(isapn)]^{2+}$) was dissolved in 99.9% DMSO to a final concentration of 17.7 mM and stored at −20 °C. Anti-FLAG M2 monoclonal affinity gel, FLAG peptide and anti-FLAG M2 monoclonal antibody were provided by Sigma-Aldrich. *Saccharomyces cerevisiae* Top1 null strain EKY3 (ura3-52, his3Δ200, leu2Δ1, trp1Δ63, top1::TRP1, MATα) was used to express the hTop1 gene. Single copy plasmid YCpGAL1-e-hTop1, in which the hTop1 is expressed under the galactose inducible promoter, was described previously [25]. The hTop1Gly717Phe was generated by oligonucleotide-directed mutagenesis of the YCpGAL1-hTop1. The epitope-tagged construct YCpGAL1-e-hTop1 contains the N-terminal sequence FLAG: DYKDDDDY (indicated with 'e'), recognized by the M2 monoclonal antibody. The epitope-tag was subcloned into YCpGAL1-hTop1Gly717Phe to produce the YCpGAL1-e-hTop1Gly717Phe.

2.2. Drug sensitivity assay

Yeast EKY3 strains were transformed with YCp50, YCpGAL1-e-hTop1 and YCpGAL1-e-hTop1Gly717Phe by LiOAc treatment and selected on synthetic complete (SC)-uracil medium supplemented with 2% dextrose. Cultures of transformants were grown to an Abs595 of 0.3 and 5 μL aliquots of serial 10-fold dilutions were spotted onto SC-uracil plates plus 2% dextrose or 2% galactose, with or without the indicated concentrations of CPT. Plates were incubated at 30 °C for 3 days.

2.3. Protein purification

The transformed EKY3 yeast cells with YCpGAL1-e-hTop1 and YCpGAL1-e-hTop1Gly717Phe were grown to an Abs595 of 1.0 on SC-uracil plus 2% dextrose. Then they were diluted 1:100 in SC-uracil plus 2% raffinose and grown overnight until Abs595 of 1.0 again. After 6 h induction with 2% galactose, the cells were then centrifuged, washed with cold water and resuspended in 2 mL TEEG buffer per gram wet cells [50 mM Tris–HCl, pH 7.4, 1 mM EDTA, 1 mM EGTA, 10% glycerol and protease inhibitors cocktail from Roche, supplemented with 0.1 mg/mL sodium bisulfate, 0.8 mg/mL sodium fluoride, 1 mM PMSF and 1 mM DTT]. The 0.5 volumes of 425–600 μm diameter glass beads were mixed with cells, the cells were disrupted by vortexing 30 times for 30 s alternating with 30 s on ice and then centrifuged for 30 min at 15,000 *g* to collect supernatant. To purify the interested protein, an anti-FLAG M2 monoclonal affinity gel (Sigma-Aldrich) was equilibrated to the columns as described in the technical protocol and washed with 20 volumes of TBS (50 mM Tris–HCl pH 7.4 and 150 mM KCl) supplemented with the protease inhibitors. Then the whole extracts were applied to the columns. 1 mg of FLAG peptide (DYKDDDDK), diluted to five column volumes of TBS buffer, was adopted to elute e-hTop1 or e-hTop1Gly717Phe protein by competition binding sites. Fractions of 500 μL were collected and stored in 40% glycerol at −20 °C. Protein levels and integrity were assessed by immunoblot with the monoclonal anti-FLAG M2 antibody as described in D'Annessa et al (2013) [20].

2.4. DNA relaxation assays

HTop1 activity was assayed with a DNA relaxation assay. Equal amount of hTop1 or hTop1Gly717Phe protein was incubated with 0.5 μg of negatively supercoiled pBlue-Script KSII(+) DNA, present in both dimeric and monomeric forms, in 30 μL of reaction buffer containing 20 mM Tris–HCl pH 7.5, 0.1 mM Na_2EDTA, 10 mM $MgCl_2$, 5 μg/mL acetylated bovine serum albumin and 150 mM KCl, in the absence and presence of CPT or oxindolimine copper(II) compound ($[Cu(isapn)]^{2+}$) recently tested as a hTop1 inhibitor [26]. Reactions were incubated at 37 °C and terminated with 0.5% SDS at each indicated time-course point. The samples were resolved at a 1% (*w*/*v*) agarose gel in running buffer containing 48 mM Tris, 45.5 mM boric acid, and 1 mM EDTA at 10 V/cm. After staining with ethidium bromide (0.5 μg/mL) and washing with water, the gels were first exposed to UV light for 30 min to induce photo-nicking of the plasmid, then stained again with ethidium bromide (0.5 μg/mL) for 20 min and photographed using a UV transilluminator [17]. The remaining supercoiled plasmid percentage, quantified using ImageJ software (http://rsbweb.nih.gov/ij/) was normalized to total amount of DNA in each lane and plotted as a function of time.

2.5. Cleavage kinetics

Oligonucleotide CL14-U (5′-GAAAAAAGACTUAG-3′) was radiolabelled with [γ 32P] ATP at its 5′-end [27]. The CP25 complementary strand (5′-TAAAAATTTTTCTAAGTCTTTTTTC-3′) was phosphorylated at its 5′-end with unlabeled ATP. The CL14-U strand was annealed with a 2-fold molar excess of CP25 to obtain the CL14-U/CP25 suicide substrate, which contains an hTop1 preferred high affinity cleavage site. Further, equal amount of hTop1 or hTop1Gly717Phe enzyme was incubated with 20 nM suicide substrate in 20 mM Tris–HCl pH 7.5, 0.1 mM Na_2EDTA, 10 mM $MgCl_2$, 5 μg/mL acetylated BSA, and 150 mM KCl, in absence or presence of 50 μM $[Cu(isapn)]^{2+}$ [26] at 25 °C. Five microlitre aliquots were removed at indicated time points and the reaction was stopped with 0.5% (*w*/*v*) SDS. The samples were directly analyzed by denaturing 7 M urea/20% polyacrylamide gel electrophoresis in running buffer containing 48 mM Tris, 45.5 mM boric acid, and 1 mM EDTA.

The percentage of cleaved substrate (Cl1) was determined by PhosphorImager and ImageQuant software and normalized to the total radioactivity amount in each lane. The cleavage experiment was not performed in the presence of CPT since it is well known that it does not affect cleavage reaction [5,10,13].

2.6. Religation kinetics

Oligonucleotide CL14 (5′-GAAAAAAGACTTAG-3′) was radiolabelled with [γ 32P] ATP at its 5′-end. The CP25 complementary strand(5′-TAAAAATTTTTCTAAGTCTTTTTTC-3′) was phosphorylated at its 5′-end with unlabeled ATP. The CL14 strand was annealed with a 2-fold molar excess of CP25 to obtain CL14/CP25 suicide substrate containing an hTop1 high affinity cleavage site. Equal amount of hTop1 or hTop1Gly717Phe enzyme was incubated with 20 nM of CL14/CP25 suicide substrate for 60 min at 25 °C plus 30 min at 37 °C in 20 mM Tris–HCl pH 7.5, 0.1 mM Na_2EDTA, 10 mM $MgCl_2$, 5 μg/mL acetylated BSA and 150 mM KCl. After the formation of the cleavage complex (Cl1), a 5 μL aliquot was removed and used as time 0 point. Subsequently, a 200-fold molar excess of R11 oligonucleotide (5′-AGAAAAATTTT-3′) over the CL14/CP25 substrate was mixed with the cleavage complex to start the religation reaction after adding the DMSO or 100 μM CPT or 50 μM $[Cu(isapn)]^{2+}$. Five microlitre aliquots were removed at indicated time points and the reaction was stopped with 0.5% (*w*/*v*) SDS. After ethanol precipitation, the samples were resuspended in 5 μl of 1 mg/mL trypsin and incubated at 37 °C for 60 min. But trypsin cannot completely digest hTop1, a trypsin resistant peptide remains attached to the substrate after digestion, which result to the 12 nt (Cl1) oligo running slower than the uncleaved in the gel. The samples were analyzed by denaturing 7 M urea/20% polyacrylamide gel electrophoresis in running buffer containing 48 mM Tris, 45.5 mM boric acid, and 1 mM EDTA. The percentage of remaining cleavage complex was quantified by ImageQuant software, divided to the total radioactivity for each lane and normalized to the value at $t = 0$, finally plotted as a function of time.

2.7. Molecular dynamics simulation

The starting coordinates for the protein and the 22 DNA bps forming the hTop1–DNA covalent complex have been derived as described in Mancini *et al.* 2010 [28]. The Gly717Phe mutation has been introduced with the leap tool of Amber 12 [29] upon topology creation. The complex has been immersed in a rectangular box and further solvated with 31,776 TIP3P water molecules [30] and neutralized by adding 20 Na^+ counter-ions, the final super script system being composed by 106,220 atoms. The simulation has been run with the GROMACS MD package version 4.5.3 [31], using the AMBER10 all-atoms force field [32] implemented in GROMACS [33].

Electrostatic interactions have been taken into account by means of the Particle Mesh Ewald method (PME) using a cutoff of 1.2 nm for the real space and Van der Waals interactions [34]. The bond lengths and angles have been constrained using the LINCS algorithm [35]. Relaxation of solvent molecules and Na^+ ions was initially performed with subsequent steps of 200 ps at 50, 100, 150, 200, and 250 K till a final temperature of 300 K. The system has been then simulated for 75 ns with a time step of 2.0 fs and the neighbors' list was updated every 10 steps. Temperature was kept constant at 300 K using the velocity rescale method with a coupling constant of 0.1 ps during sampling, while pressure was kept constant at 1 bar using the Parrinello–Rahman barostat with a coupling constant of 1.0 ps during sampling [36].

All the analyses presented here refer to the last 72 ns, where the first 3 ns has been considered as equilibration and has been performed in comparison with a simulation of the wild type enzyme previously performed [37]. The analyses have been carried out with the GROMACS package 4.5.3 [31], graphs have been obtained with the Grace program (http://plasma-gate.weizmann.ac.il/Grace/) and images were created using the VMD [38].

3. Results

3.1. The Gly717Phe mutant is resistant to CPT when expressed in yeast cells

The Gly717Phe mutant has been introduced in the single copy yeast plasmid (YCp) expressing the hTop1 under the GAL1 promoter. To exclude the interference of the Top1 produced by cell itself, a Top1Δ yeast strain (EKY3) is adopted to express the hTop1 gene. The *in vivo* activity comparison of the wild type and the Gly717Phe mutant has been assessed in five independent viability assays on EKY3 transformed with GAL1-hTop1 constructs (Fig. 1). Serial dilutions of each transformed yeast cell were spotted on plates containing dextrose, galactose and galactose supplemented with different CPT concentrations to assess drug sensitivity following the yeast growth. The data show that yeast cells expressing the wild type protein exhibit a deficiency in viability in the presence of 10 ng/mL CPT, while the Gly717Phe mutant displays viable colonies up to a CPT concentration of 100 ng/mL (Fig. 1). These results indicate that the Gly717Phe mutant is resistant to the drug *in vivo*.

3.2. The mutant Gly717Phe is resistant to CPT in vitro

The catalytic activity of the wild type and Gly717Phe mutant has also been tested *in vitro* in the absence and presence of 100 μM CPT (Fig. 2). A time course experiment was carried out considering equal amounts of purified wild type and Gly717Phe proteins in the presence of supercoiled plasmid DNA, from 0.25 to 60 min. In the absence of CPT the same volume of DMSO is used to show that the solvent doesn't affect the relaxation activity of the two enzymes. The reaction products have been resolved by agarose gel electrophoresis. The supercoiled DNA is completely relaxed by the wild type as well as the mutant after 2 min (Fig. 2A lane 5, Fig. 2B full black and gray line), however, the relaxation rate is slowed down with varying degrees in the presence of CPT. In detail, CPT decreases the relaxation of the supercoiled substrate by the wild type up to 15 min (Fig. 2A lane 17, Fig. 2B dashed black line), while in the case of the Gly717Phe mutant the decrease is observed only up to 4 min (Fig. 2A lane 15, Fig. 2B dashed gray line), indicating that the mutant is partially resistant to CPT also *in vitro*.

3.3. Cleavage kinetics of the wild type and Gly717Phe mutant

The time course of the cleavage of the wild type and Gly717Phe mutant has been followed using a suicide cleavage substrate. In detail, a 5′-end radiolabelled oligonucleotide CL14-U (5′-GAAAAAAGACTUAG-3′) with a ribo-Uracil (rU) in position 12 has been annealed to a CP25 (5′-TAAAAATTTTTCTAAGTCTTTTTTC-3′) complementary strand, to produce a duplex with a 11-base 5′-single-strand extension, as shown in the top of Fig. 3A, where the arrow indicates the preferred cleavage site. After the nick, the 2′-OH of the ribose can attack the 3′-phosphotyrosyl linkage between the enzyme and ribonucleotide, leading to the hTop1 release and leaving a 2′,3′-cyclic phosphate. Incubation of an excess of the wild type and mutated enzyme gives rise to the band distribution observed in Fig. 3A normalized to the total radioactivity amount in each lane and plotted as a function of time, evidences that the wild type and the Gly717Phe mutant protein have the same rate of cleavage and reach the same plateau value (Fig. 3B).

3.4. Religation kinetics of the wild type and Gly717Phe mutant

The religation reaction has been carried out incubating an excess of wild type or mutant enzymes with the suicide substrate to allow the cleavage to proceed to completion and adding a 200-fold molar excess of complementary R11 oligonucleotide (5′-AGAAAAATTTT-3′) in the absence and presence of CPT. Aliquots have been removed at different times and analyzed on urea-polyacrylamide gel (Fig. 4A). The percentage of the remaining cleavage complex (Cl1) has been quantified,

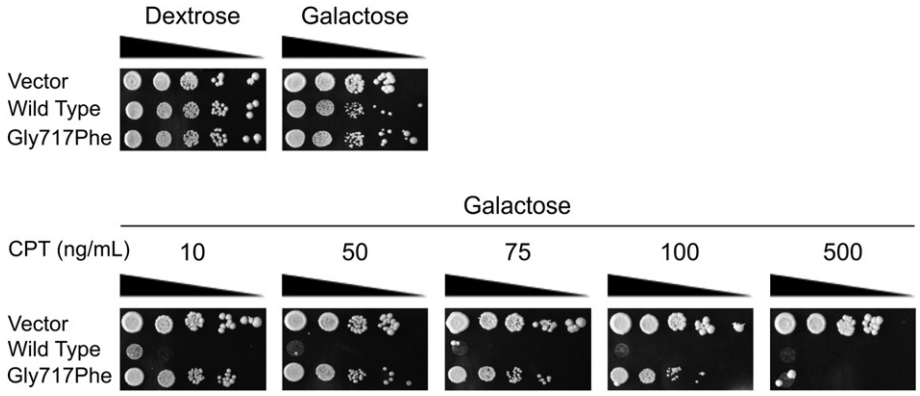

Fig. 1. Drug sensitivity assay of transformed yeast cells. Exponential cultures of yeast cells were transformed with vector YCp, YCpGAL1-hTop1 and YCpGAL1-hTop1Gly717Phe were serially 10-fold diluted and spotted onto SC-uracil plates supplemented with dextrose, galactose or galactose and the indicated CPT concentrations.

normalized to the time 0 and plotted in Fig. 4B. The religation rate of the native enzyme is inhibited in the presence of CPT (compare the black full line with the black dotted line). The Gly717Phe mutant has a religation rate faster than the wild type protein (compare the black full line with the gray full line) and the rate doesn't change in the presence of CPT (compare the black dashed line and the gray full line with the gray dashed line) indicating that the mutant maintains an efficient religation even in the presence of the drug.

3.5. Dynamical–structural effect of the 717 residue mutation

A 75 ns molecular dynamics simulation of the Gly717Phe mutant in covalent complex with a 22 DNA bps has been analyzed in comparison to the one of the wild type enzyme previously performed [37]. The two proteins share a comparable fluctuation profile, as shown by the plot of the per-residue Root Mean Square Fluctuation (RMSF) (Fig. 5), with the main differences at the level of the linker domain and in the nearby

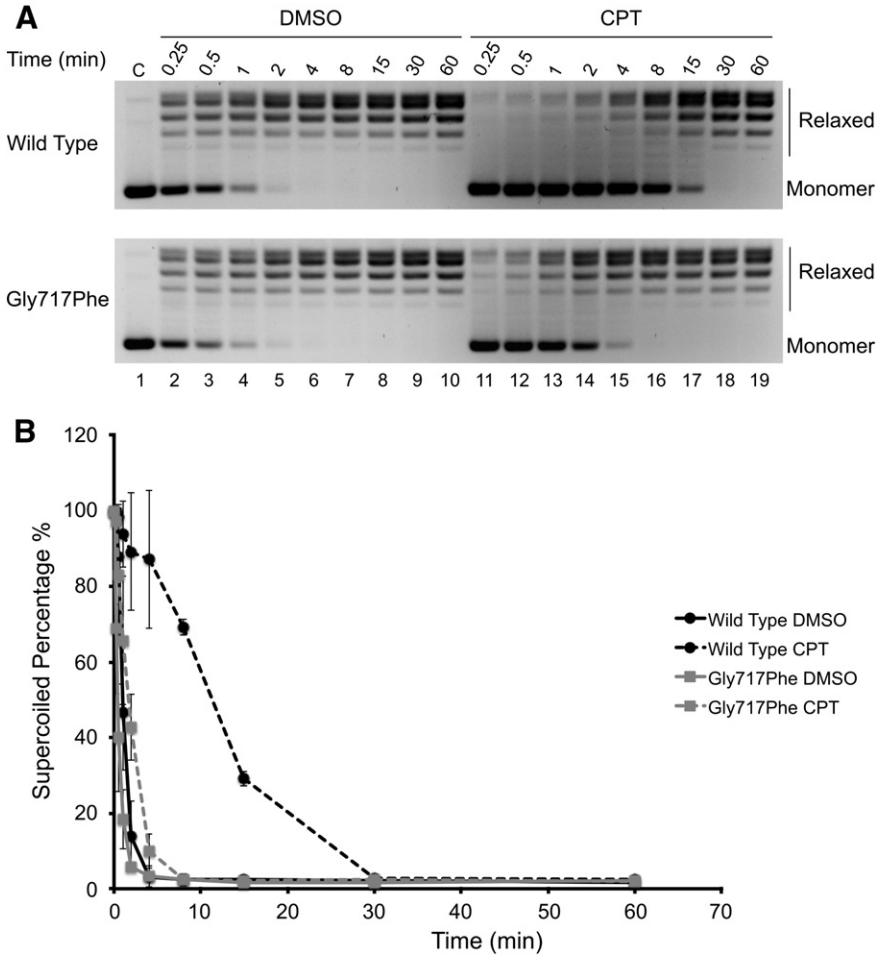

Fig. 2. Time course relaxation assay. (A) Equal amount of hTop1 or Gly717Phe was incubated with a negative supercoiled plasmid for each indicated time-course point in the presence of DMSO (lanes 2–10) or 100 μM CPT (lanes 11–19). C, no protein added (lane 1). The two forms of the plasmid DNA were indicated as "Monomer" and "Relaxed". The reaction products were resolved in agarose gel and visualized after staining with ethidium bromide. (B) Percentage of supercoiled plasmid, relative to the total amount of DNA for each lane, plotted against time in the absence or in the presence of CPT for the wild type (dots, full and dashed black lines, respectively) and the Gly717Phe mutant (squares, full and dashed gray lines, respectively). Three independent experiments were performed to obtain the average value and the standard deviation.

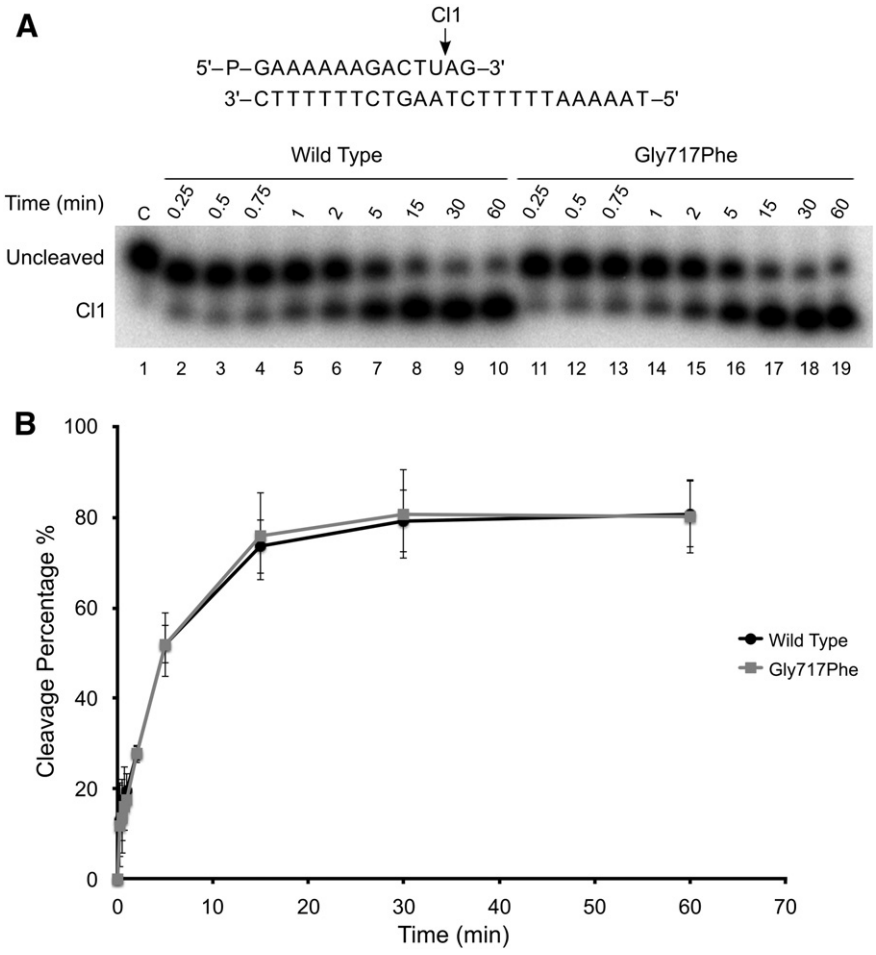

Fig. 3. Cleavage kinetics. (A) Time course of the cleavage reaction of purified wild type (lanes 2–10) and Gly717Phe mutant (lanes 11–19) carried out with the CL14-U/CP25 substrate described at the top of the figure. C, no protein added (lane 1). Cl1 identifies the cleaved strand by the enzymes at the preferred cleavage site, indicated by an arrow at the top of the figure. (B) Percentage of the appearance of the cleaved fragment, normalized to the total radioactivity amount in each lane, plotted against time for the reaction with the wild type (black dots) or the Gly717Phe mutant (gray squares). Three independent experiments were performed to obtain average value and the standard deviation for error bar.

residues. In the mutant the linker domain has a lower fluctuation when compared to the wild type, while the flanking regions of the inker, residues 633–656 and 698–719, increase their mobility (Fig. 5). The RMSF plot also evidences a difference in the fluctuation profile of residue Glu497, which has been shown in the X-ray structure to form a salt bridge with Lys369 crucial for the maintenance of the protein clamp around the DNA [3]. This residue is less fluctuating in the Gly717Phe mutant, and indeed the salt bridge with the lysine is highly stable, being present for the 100% of total simulation time instead of 35% as in the wild type. The linker displays a reduced flexibility in the mutant that is reflected by a limited conformational space sampled by the domain, as indicated by a cluster analysis (Fig. 6A) carried out on the Cα atoms of residues Ala625–Lys712, using a cut off of 5 Å and fitting the structure on the Cα atoms of the remaining residues (201–624, 713–765). The procedure gives rise to 16 clusters for the wild type and 4 for the mutant. In the first case the first 4 clusters contain 59%, 19%, 9% and 5% of the total conformations, respectively, while in the case of the mutant the first cluster contains 99% of the total conformations. This indicates that in the mutant not only the linker is less fluctuating but that its motion is restricted in a very limited space (Fig. 6A).

The principal component analysis (PCA) also evidences that the main direction of the motion of the domain is different in the two proteins. Fig. 6B shows the projection of the motion along the first eigenvector that is mainly represented by the linker mobility in both systems. Taking the wild type as a reference it can be appreciated that the linker domain in the mutant undergoes a displacement from its position and that it completely changes the orientation of its oscillation causing a complete rearrangement of the interaction with the DNA (Fig. 6B). In the wild type two residues, present in the loop connecting the linker with subdomain III, interact with the DNA, His632 of the catalytic pentad with the guanine in position +2 downstream the cleavage site (Thy-1) for 75% of the simulation and Arg634 with Gua + 2 and Ade + 3 for the 80% and 60% of total simulation time, respectively. Due to the change in orientation of the linker the three interactions are lost in the mutant, similarly to what has been observed in the Arg634Ala mutant, which is also characterized by an altered linker mobility and CPT sensitivity [20].

3.6. Effect of the mutation on the structure of helix 20 and the active site architecture

The Gly717 mutated residue, is located on the loop connecting helix 19, the second helix of the linker domain, and helix 20, the first helix of the C-terminal domain, also harboring the active site residue Tyr723 (Fig. S1). The mutation has a structural–dynamical effect on the bundle of helices formed by helices 16, 17, 19, 20 and 21. The bundle in the Gly717Phe mutant is less compact, as indicated by the gyration radius plotted along the trajectory (data not shown) that reaches a final value of 14.8 Å compared to 13.8 Å in the wild type. The loss in compactness is reflected by a weaker interaction between the helices (Fig. S2), as observed in the case of the Thr729Lys and Glu710Lys mutants, both displaying CPT resistance [21,22].

The proximity of the mutation to the active site affects the architecture of the catalytic pentad, as evidenced by the comparison of

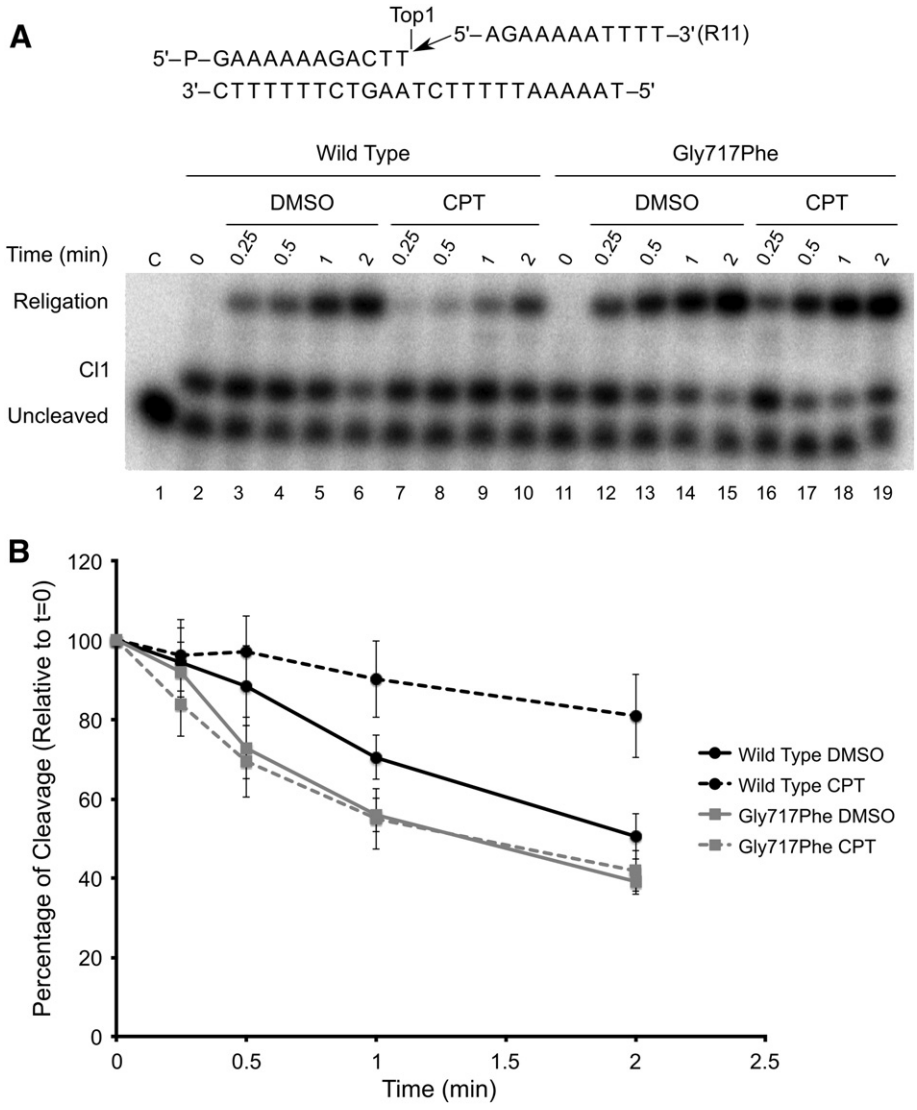

Fig. 4. Religation kinetics. (A) Time course of the religation experiment of R11 complementary substrate (shown at the top of the figure) carried out with the wild type or Gly717Phe mutant covalent cleaved complexes in absence (lanes 3–6 and lanes 12–15 for wild type and Gly717Phe mutant respectively) or in the presence of 100 μM CPT (lanes 7–10 for the wild type and lanes 16–19 for Gly717Phe mutant). C, no protein added (lane 1). Time 0 represents the completely cleaved substrate before the addition of the R11 strand for the wild type (lane 2) and the Gly717Phe mutant (lane 11). Cl1 indicates the peptide covalent cleaved complexes formed at the preferred reaction site. (B) Percentage of the disappearance of the cleaved fragment, normalized to the time 0, plotted against time for the wild type in the presence of DMSO (full black line) or CPT (dashed black line) and for the Gly717Phe mutant in the presence of DMSO (full gray line) or CPT (dashed gray line). Three independent experiments were performed to obtain the average value and the standard deviation for error bar.

the hydrogen bond network established by the pentad with the surrounding residues in the two proteins (Table 1). A large decrease in the number of interactions is detected in the mutant, affecting the architecture of the active site, and several hydrogen bonds important for the correct binding of the drug are lost as described in the scheme reported in Fig. 7. In detail, in the mutant the Lys532–Asp533 and the Tyr723–Asn722 hydrogen bounds, present for more than 95% of the total simulation time in the wild type, are present for 34% in the first case and completely lost in the second one. Residues Asp533 and Asn722 are involved in the stabilization of CPT through direct or water mediated interactions [10], suggesting that the different network of hydrogen bonds may have an effect on the drug stabilization so explaining the reduced CPT sensitivity displayed by the mutant.

3.7. Effect of the $[Cu(isapn)]^{2+}$ compound on the wild type and Gly717Phe mutant

For supporting the hypothesis that the mutation bringing CPT resistance is correlated to the rearrangement of the residues close to the active site and likely to the rearrangement of Asp533 and Asn722 involved in the stabilization of CPT, we have carried out activity assays in the presence of $[Cu(isapn)]^{2+}$ compound that was investigated for its inhibitory effect in a previous work [26]. As shown in Fig. S3A the supercoiled DNA is completely relaxed by the wild type as well as by the mutant after 4 min in the presence of DMSO (Fig. S3A, lane 6). Addition of 50 μM $[Cu(isapn)]^{2+}$ fully inhibits the relaxation reaction until 60 min for both enzymes (Fig. S3A, lane 19) indicating an identical inhibition mechanism. As confirmed by the plot as a function of time of the supercoiled plasmid percentage, normalized to total amount of DNA for each lane (Fig. S3B). The cleavage rate carried out in the presence of 50 μM $[Cu(isapn)]^{2+}$, is inhibited for both the wild type and the Gly717Phe mutant (Fig. S4A) by an identical extent, as confirmed by the quantitative plot (Fig. S4B) again suggesting a similar inhibitory mechanism. Finally a similar partial inhibition is also observed at the level of the religation rate (Fig. S5A and S5B). The Gly717Phe mutant has a religation rate faster than the wild type protein (compare the black full line with the gray full line), but the copper compound inhibits at the same extent both the wild type protein

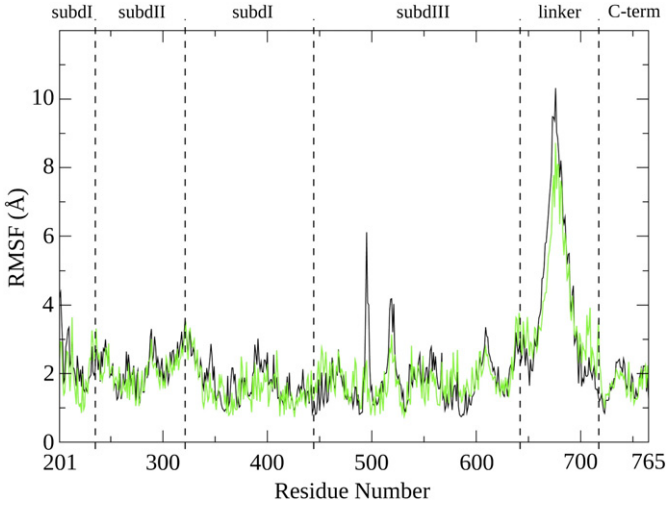

Fig. 5. Analysis of residues' fluctuation. Per-residue root mean square fluctuation of the Gly717Phe mutant vs the wild type (gray and black line, respectively). The domain division of the protein is also reported.

Table 1
Percentage of the hydrogen bonds established by the active site pentad with the surrounding residues. Only the interactions present for more than 60% of total simulation time in at least one of the two trajectories are reported. The interactions conserved between the two simulations are reported in bold.

Active site residues	Interactors	Wild type	Gly717Phe
Arg488	**Tyr537**	64.32	79.14
	Asn631	–	68.17
	Cys504	99.17	68.26
	Tyr723	99.55	–
Lys532	Asp533	96.27	33.59
	Ser534	84.78	–
	Ile535	59.43	83.38
Arg590	Ala586	17.13	72.39
	Lys587	87.51	–
	Asn593	69.65	–
	Ala594	96.66	90.50
	Tyr723	96.52	16.79
His632	**Ala627**	90.03	95.94
	Cys630	76.16	–
	Asn631	63.66	–
	Ala715	–	89.99
	Tyr723	–	70.72
Tyr723	**Ser719**	96.73	86.75
	Asn722	99.99	–

and the Gly717Phe mutant (compare the black dash line with the gray dash line in Figure S5B).

4. Discussion

In this study we have characterized the Gly717Phe mutant located in a loop preceding helix 20 formed by residues 718–723 (Fig. S1). The combined functional and computational approach allowed us to characterize the effect of the mutation on the structural, dynamical and functional properties. In detail, a viability assay carried out on yeast cells, where the endogenous Top1 has been deleted and the human Gly717Phe mutant Top1 has been expressed, indicates that the cells are able to grow also in the presence of CPT (Fig. 1), demonstrating CPT resistance. The wild type and the mutated enzymes are characterized by the same cleavage rate (Fig. 3) but the mutant displays a religation rate faster than wild type and the rate is not affected by CPT (Fig. 4), suggesting that drug resistance is due to the fast religation kinetics. Molecular dynamics simulation of the mutant in comparison with the wild type highlights that the main differences between the systems are at the level of the linker domain and the active site. The linker displays a different profile of fluctuation, showing a lowered mobility at the tip of the domain and a slightly higher motion at the N- and C-terminus (Fig. 5). The perturbed mobility of the linker can be better appreciated by the cluster analysis showing that the domain is more rigid and samples a confined conformational space (Fig. 6A). Indeed the domain completely changes its orientation toward the DNA double helix as shown by the PCA study (Fig. 6B). Moreover proteolysis experiment (data not shown) suggests that the mutation does not strongly perturb the domain organization. All together these data suggest that the mutation influences the ability of the linker to guide the DNA during the strand rotation affecting the religation kinetics (Fig. 4). The mutation also has a direct effect on the active site, which in the mutant has a slight different three-dimensional arrangement, due to a different network of hydrogen bonds with the nearby residues (Table 1 and Fig. 7). The new network of hydrogen bonds established by the mutant lacks the two Lys532–Asp533 and Tyr723–Asn722 interactions, involving Asp533 and Asn722, known to play a key role in the CPT binding [10,28]. The different profile of interaction of the two residues may be one of the causes for the decreased stabilization of the drug that can explain the CPT resistance. Meanwhile, a non-CPT inhibitor, the copper compound $[Cu(isapn)]^{2+}$ that likely acts coordinating with Glu492 and Asp563 residues shows an identical inhibitory effect both on the wild type and Gly717Phe mutant supporting the hypothesis that the CPT resistance observed for the mutant is in part due to a rearrangement of the residues close to the active site including residues Asp533 and Asn722 that in the wild type are involved in the stabilization of CPT [10].

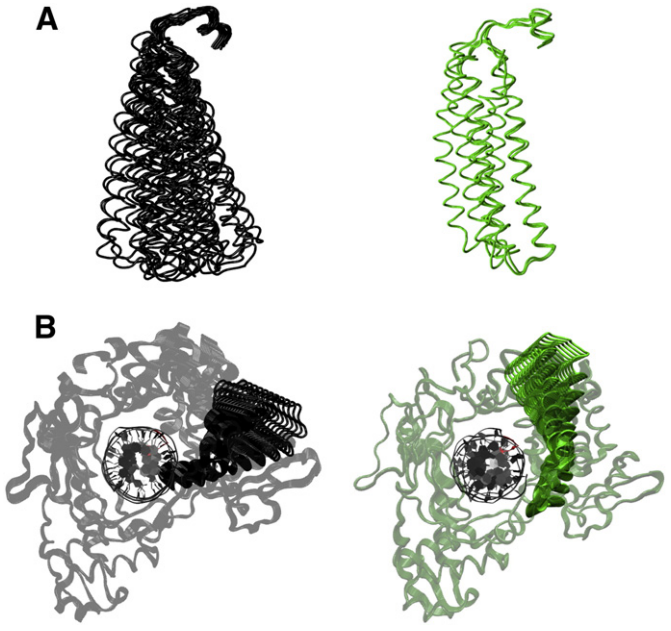

Fig. 6. Linker's motion. (A) Centroids of the families obtained with the cluster analysis for the linker of the wild type (black) and the Gly717Phe mutant (green). (B) Projection of the motion along the first eigenvector for the wild type (black) and the Gly717Phe mutant (green). The core and C-terminal domains are reported in transparent in order to better appreciate the linker behavior. The two systems are oriented in the same way, as can be seen also by the −1 base highlighted in red.

It is interesting to remark that CPT resistance has been also previously reported in the Gly721Phe mutant of the yeast enzyme, involving Gly721 corresponding to the human Gly717 [24]. In that study the authors suggest that the resistance could be due to an enhanced flexibility of the linker domain, basing their hypothesis on the position of Gly721 that could act as a hinge for the mobility of the domain. Here we propose that in the human enzyme the resistance is correlated to a perturbation in the linker, the main effect being a change in its orientation toward the DNA substrate and a slight rearrangement of the active

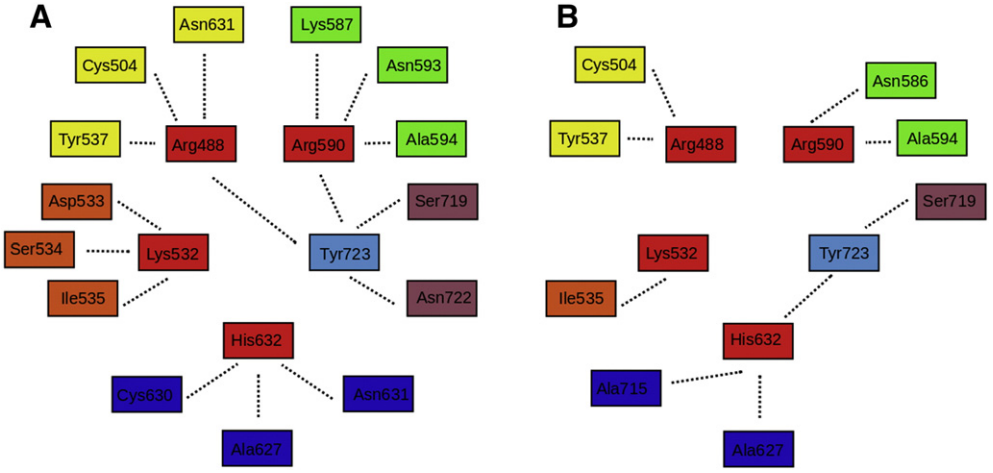

Fig. 7. Schematic representation of the hydrogen bond network involving the catalytic pentad residues in the wild type (A) and the Gly717Phe mutant (B). The residues of the pentad are shown in red (Arg480, Lys532, Arg590 and His632) and light blue (Tyr723). The connections between the residues are represented by a dashed line that is present when a hydrogen bond persists for more than 60% of total simulation time.

site (Fig. 6 and 7 and Table 1). These data confirm the importance of the linker in modulating drug reactivity as initially demonstrated by a study in which the enzyme deleted of the linker domain displayed an increase in the religation rate and a decrease in CPT sensitivity [5] and further demonstrated in single and double mutants (Ala653Pro, Thr718Ala, Lys681Ala and Asp677Gly–Val703Ile), showing a correlation between linker flexibility and CPT reactivity [17–19,23]. Such a correlation has been confirmed on a chimeric enzyme constituted by the human enzyme containing the linker from *Plasmodium falciparum* Top1 [27]. However, CPT resistance has been also reported in mutants having a low degree of correlation between the linker and the C-terminal domain, as shown in the Glu710Gly, Arg634Ala and Thr729Lys/Pro mutants [20–22]. In this work we confirm the importance of the linker, being the drug resistance coupled to a reorientation of the domain motion that modulates its interaction with the DNA, likely affecting the strand rotation, and by a slight rearrangement of the residues close to the active site involved in the CPT stabilization. Moreover, this study shows that Gly717 and Gly721, in the human and yeast enzyme, play an identical role since in both enzymes mutation to Phe gives rise to a CPT resistant phenotype.

Supplementary data to this article can be found online at http://dx.doi.org/10.1016/j.bbapap.2015.04.017.

Conflict of interest

The authors declare no competing financial interest.

Acknowledgments

This work was supported by Associazione Italiana Ricerca Cancro (AIRC) with the project N. 10121 and by a scholarship to Zhenxing Wang from Erasmus Mundus Action 2 TECHNO project. The authors thank Fabio Retico for the help in obtaining the simulation of the mutant.

References

[1] K.D. Corbett, J.M. Berger, Structure, molecular mechanisms, and evolutionary relationships in DNA topoisomerases, Annu. Rev. Biophys. Biomol. Struct. 33 (2004) 95–118.
[2] J.C. Wang, Cellular roles of DNA topoisomerases: a molecular perspective, Nat. Rev. Mol. Cell Biol. 3 (2002) 430–440.
[3] J.J. Champoux, DNA topoisomerases: structure, function, and mechanism, Annu. Rev. Biochem. 70 (2001) 369–413.
[4] L. Stewart, G.C. Ireton, L.H. Parker, K.R. Madden, J.J. Champoux, Biochemical and biophysical analyses of recombinant forms of human topoisomerase I, J. Biol. Chem. 271 (1996) 7593–7601.
[5] L. Stewart, G.C. Ireton, J.J. Champoux, A functional linker in human topoisomerase I is required for maximum sensitivity to camptothecin in a DNA relaxation assay, J. Biol. Chem. 274 (1999) 32950–32960.
[6] M.R. Redinbo, J.J. Champoux, W.G. Hol, Novel insights into catalytic mechanism from a crystal structure of human topoisomerase I in complex with DNA, Biochemistry 39 (2000) 6832–6840.
[7] M.R. Redinbo, L. Stewart, J.J. Champoux, W.G. Hol, Structural flexibility in human topoisomerase I revealed in multiple non-isomorphous crystal structures, J. Mol. Biol. 292 (1999) 685–696.
[8] M.R. Redinbo, L. Stewart, P. Kuhn, J.J. Champoux, W.G. Hol, Crystal structures of human topoisomerase I in covalent and noncovalent complexes with DNA, Science 279 (1998) 1504–1513.
[9] B.L. Staker, K. Hjerrild, M.D. Feese, C.A. Behnke, A.B. Burgin Jr., L. Stewart, The mechanism of topoisomerase I poisoning by a camptothecin analog, Proc. Natl. Acad. Sci. U. S. A. 99 (2002) 15387–15392.
[10] B.L. Staker, M.D. Feese, M. Cushman, Y. Pommier, D. Zembower, L. Stewart, A.B. Burgin, Structures of three classes of anticancer agents bound to the human topoisomerase I–DNA covalent complex, J. Med. Chem. 48 (2005) 2336–2345.
[11] Y.H. Hsiang, L.F. Liu, Identification of mammalian DNA topoisomerase I as an intracellular target of the anticancer drug camptothecin, Cancer Res. 48 (1988) 1722–1726.
[12] Y. Pommier, Topoisomerase I inhibitors: camptothecins and beyond, Nat. Rev. Cancer 6 (2006) 789–802.
[13] Y.H. Hsiang, M.G. Lihou, L.F. Liu, Arrest of replication forks by drug-stabilized topoisomerase I-DNA cleavable complexes as a mechanism of cell killing by camptothecin, Cancer Res. 49 (1989) 5077–5082.
[14] A. Tanizawa, R. Beitrand, G. Kohlhagen, A. Tabuchi, J. Jenkins, Y. Pommier, Cloning of Chinese hamster DNA topoisomerase I cDNA and identification of a single point mutation responsible for camptothecin resistance, J. Biol. Chem. 268 (1993) 25463–25468.
[15] P. Benedetti, P. Fiorani, L. Capuani, J.C. Wang, Camptothecin resistance from a single mutation changing glycine 363 of human DNA topoisomerase I to cysteine, Cancer Res. 53 (1993) 4343–4348.
[16] J.E. Chrencik, B.L. Staker, A.B. Burgin, P. Pourquier, Y. Pommier, L. Stewart, M.R. Redinbo, Mechanisms of camptothecin resistance by human topoisomerase I mutations, J. Mol. Biol. 339 (2004) 773–784.
[17] P. Fiorani, A. Bruselles, M. Falconi, G. Chillemi, A. Desideri, P. Benedetti, Single mutation in the linker domain confers protein flexibility and camptothecin resistance to human topoisomerase I, J. Biol. Chem. 278 (2003) 43268–43275.
[18] I. D'Annessa, C. Tesauro, P. Fiorani, G. Chillemi, S. Castelli, O. Vassallo, G. Capranico, A. Desideri, Role of flexibility in protein–DNA–drug recognition: the case of Asp677Gly–Val703Ile topoisomerase mutant hypersensitive to camptothecin, J. Amino Acids 2012 (2012) 206083.
[19] P. Fiorani, C. Tesauro, G. Mancini, G. Chillemi, I. D'Annessa, G. Graziani, L. Tentori, A. Muzi, A. Desideri, Evidence of the crucial role of the linker domain on the catalytic activity of human topoisomerase I by experimental and simulative characterization of the Lys681Ala mutant, Nucleic Acids Res. 37 (2009) 6849–6858.
[20] I. D'Annessa, C. Tesauro, Z. Wang, B. Arno, L. Zuccaro, P. Fiorani, A. Desideri, The human topoisomerase 1B Arg634Ala mutation results in camptothecin resistance and loss of inter-domain motion correlation, Biochim. Biophys. Acta 1834 (2013) 2712–2721.
[21] C. Tesauro, B. Morozzo Della Rocca, A. Ottaviani, A. Coletta, L. Zuccaro, B. Arno, I. D'Annessa, P. Fiorani, A. Desideri, Molecular mechanism of the camptothecin resistance of Glu710Gly topoisomerase IB mutant analyzed in vitro and in silico, Mol. Cancer 12 (2013) 100.

[22] G. Chillemi, I. D'Annessa, P. Fiorani, C. Losasso, P. Benedetti, A. Desideri, Thr729 in human topoisomerase I modulates anti-cancer drug resistance by altering protein domain communications as suggested by molecular dynamics simulations, Nucleic Acids Res. 36 (2008) 5645–5651.
[23] G. Chillemi, P. Fiorani, S. Castelli, A. Bruselles, P. Benedetti, A. Desideri, Effect on DNA relaxation of the single Thr718Ala mutation in human topoisomerase I: a functional and molecular dynamics study, Nucleic Acids Res. 33 (2005) 3339–3350.
[24] M. van der Merwe, M.A. Bjornsti, Mutation of Gly721 alters DNA topoisomerase I active site architecture and sensitivity to camptothecin, J. Biol. Chem. 283 (2008) 3305–3315.
[25] M.A. Bjornsti, P. Benedetti, G.A. Viglianti, J.C. Wang, Expression of human DNA topoisomerase I in yeast cells lacking yeast DNA topoisomerase I: restoration of sensitivity of the cells to the antitumor drug camptothecin, Cancer Res. 49 (1989) 6318–6323.
[26] P. Katkar, A. Coletta, S. Castelli, G.L. Sabino, R.A. Alves Couto, A.M. da Costa Ferreira, A. Desideri, Effect of oxindolimine copper(II) and zinc(II) complexes on human topoisomerase 1 activity, Metallomics 6 (2014) 117–125.
[27] B. Arno, I. D'Annessa, C. Tesauro, L. Zuccaro, A. Ottaviani, B. Knudsen, P. Fiorani, A. Desideri, Replacement of the human topoisomerase linker domain with the plasmodial counterpart renders the enzyme camptothecin resistant, PLoS One 8 (2013) e68404.
[28] G. Mancini, I. D'Annessa, A. Coletta, N. Sanna, G. Chillemi, A. Desideri, Structural and dynamical effects induced by the anticancer drug topotecan on the human topoisomerase I–DNA complex, PLoS One 5 (2010) e10934.
[29] D.A. Case, T.E. Cheatham 3rd, T. Darden, H. Gohlke, R. Luo, K.M. Merz Jr., A. Onufriev, C. Simmerling, B. Wang, R.J. Woods, The Amber biomolecular simulation programs, J. Comput. Chem. 26 (2005) 1668–1688.
[30] W.L. Jorgensen, J. Chandrasekhar, J.D. Madura, R.W. Impery, M.L. Klein, Comparison of simple potential functions for simulating liquid water, J. Chem. Phys. 79 (1983) 926–935.
[31] B. Hess, C. Kutzner, D. van der Spoel, E. Lindahl, GROMACS 4: algorithm for highly efficient, load-balanced, and scalable molecular simulation, J. Chem. Theory Comput. 4 (2008) 435–447.
[32] Y. Duan, C. Wu, S. Chowdhury, M.C. Lee, G. Xiong, W. Zhang, R. Yang, P. Cieplak, R. Luo, T. Lee, J. Caldwell, J. Wang, P. Kollman, A point-charge force field for molecular mechanics simulations of proteins based on condensed-phase quantum mechanical calculations, J. Comput. Chem. 24 (2003) 1999–2012.
[33] E.J. Sorin, V.S. Pande, Exploring the helix–coil transition via all-atom equilibrium ensemble simulations, Biophys. J. 88 (2005) 2472–2493.
[34] T.E. Cheatham, J.L. Miller, T. Fox, T.A. Darden, P.A. Kollman, Molecular-dynamics simulations on solvated biomolecular systems: the particle mesh Ewald method leads to stable trajectories of DNA, RNA, and proteins, J. Am. Chem. Soc. 117 (1995) 4193–4194.
[35] J.P. Ryckaert, G. Ciccotti, H.J.C. Berendsen, Numerical integration of the Cartesian equations of motion of a system with constraints: molecular dynamics of n-alkanes, J. Comput. Phys. 23 (1977) 327–341.
[36] M. Parrinello, A. Rahman, Polymorphic transitions in single-crystals: a new molecular-dynamics method, J. Appl. Phys. 52 (1981) 7182–7190.
[37] G. Mancini, I. D'Annessa, A. Coletta, G. Chillemi, Y. Pommier, M. Cushman, A. Desideri, Binding of an indenoisoquinoline to the topoisomerase–DNA complex induces reduction of linker mobility and strengthening of protein–DNA interaction, PLoS One 7 (2012) e51354.
[38] W. Humphrey, A. Dalke, K. Schulten, VMD—visual molecular dynamics, J. Mol. Graph. 14 (1996) 33–38.